Full Paper

Applied Organometallic Chemistry

Received: 3 July 2012 Accepted: 15 July 2012 Published online in Wiley Online Library

(wileyonlinelibrary.com) DOI 10.1002/aoc.2912

Nitrile-functionalized Hg(II)- and Ag(I)-*N*-heterocyclic carbene complexes: synthesis, crystal structures, nuclease and DNA binding activities

Rosenani A. Haque[a]*, Srinivasa Budagumpi[a], Sze Yii Choo[a], Mei Kee Choong[a], Bhadravathi Eswara Lokesh[b] and Kumar Sudesh[b]

Various nitrile-functionalized benzimidazol-2-ylidene carbene complexes of Hg(II) and Ag(I) were synthesized by the interaction of 1-benzyl/1-butyl-3-(cyano-benzyl)-3 *H*-benzimidazol-1-ium mono/dihexafluorophosphate with $Hg(OAc)_2$/Ag_2O in acetonitrile. Two of the benzimidazolium salts were structurally characterized by single crystal X-ray diffraction technique. Structures of reported compounds were characterized by ^1H, ^{13}C NMR, FT-IR, UV–visible spectroscopic techniques, and molar conductivity and elemental analyses. For bis-benzimidazolium salt, dinuclear Hg(II)– and Ag(I)–carbene complexes were obtained. Nuclease activity and binding interactions of the synthesized benzimidazolium salts and their Ag(I)–carbene complexes with DNA were studied using agarose gel electrophoresis and, absorption spectroscopy and viscosity measurements, respectively. Ag(I)–carbene complexes showed higher DNA binding activity compared to their respective benzimidazolium salts. However, a benzimidazolium salt and two of the Ag(I) complexes showed remarkably higher nuclease activity both, in the presence and absence of an oxidizing agent. Copyright © 2012 John Wiley & Sons, Ltd.

Keywords: Ag(I)–carbene complex; DNA binding; Hg(II)–carbene complex; *N*-heterocyclic carbene; nuclease activity; X-ray diffraction

Introduction

The chemistry of *N*-heterocyclic carbenes (NHCs) is centred on the availability of a lone pair of electrons on a carbene carbon atom, and its reactivity towards electropositive metal ions in forming new bonds.[1,2] NHC derivatives have a major structural difference from their phosphine analogues, and thus their physical and chemical behaviours. Since NHC ligands act as excellent σ donors and generally weak π acceptors, they can produce stable metal–NHC complexes with strong metal–carbon bonds (Chart 1). Nitrile-functionalized NHCs are potential multidentate ligands, which can give rise to carbene complexes with increased stability through ligand chelation. Their reactivity towards Ag(I) or Hg(II) is interesting and also important, especially on the mode of chelation. This field of functionalized NHC chemistry is currently of great interest and activity because of the versatile potential applications of derived complexes.[3,4]

NHCs with functionalized imidazole core are relatively common; however, those with nitrile-functionalized benzimidazole derived NHCs still remain relatively unexplored.[5,6] The choice of functional group is also crucial; this modification can be easily achieved by introducing functionalized aliphatic or aromatic groups at the nitrogen atoms of the benzimidazole ring. Although many functionalized carbene complexes were reported, nitrile-functionalized Hg(II)–NHC complexes are still very few. Recently, pyridine-derived pincer complexes of Hg(II) based on NHCs have attracted great attention as carbene transfer agents.[7] Moreover, the fluorescent emission property of an anthracene-derived Hg(II)–NHC complex is found to be stronger than that of its corresponding Ag(I)–NHC complex.[8]

In the past few years, functionalized NHCs have found application in Ag(I)–carbene complexes and their potential in transmetallation reactions has greatly increased. Functionalized Ag(I)–NHC organometallic chemistry is a well-established and flourishing field of research, especially in biomedical and nanomaterial sciences. In particular, for the possible treatment of chronic lung infections and cystic fibrosis, and perhaps even in the treatment of different types of cancer.[9–11] This biological and/or pharmaceutical relevance of Ag(I)–NHC complexes has promoted the synthesis of model silver compounds containing functionalized NHC ligands. The stability of the central bioactive benzimidazole core has inspired medicinal chemists to synthesize new potential Ag(I)–NHC complexes to explore their anticancer potential.[12–14] Furthermore, their high stability and ease of derivatization make them suitable compounds for drug discovery and development.

On the other hand, the interaction of Ag(I)–NHC complexes with DNA is a major area of research to be explored to a greater extent due to the utility of these carbene complexes in the development of spectroscopic probes, diagnostic agents and site-specific nucleic acid cleavers, among others.[15] Ag(I)–NHC complexes would be valuable in the rational design of sequence-specific DNA binding

* *Correspondence to: Rosenani A. Haque, The School of Chemical Sciences, Universiti Sains Malaysia, 11800 USM, Penang, Malaysia. E-mail: rosenani@usm.my*

a *The School of Chemical Sciences, Universiti Sains Malaysia, 11800 USM, Penang, Malaysia*

b *Ecobiomaterial Research Laboratory, The School of Biological Sciences, Universiti Sains Malaysia, 11800 USM, Penang, Malaysia*

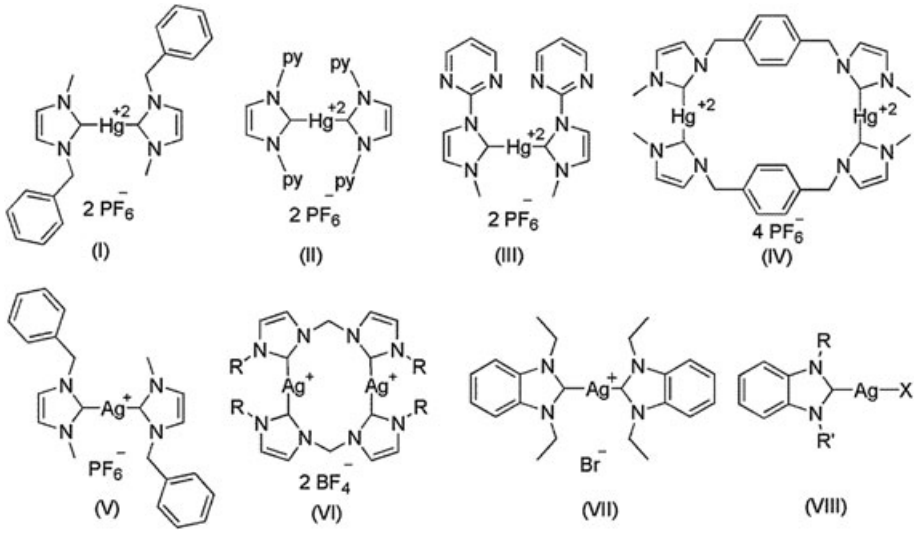

Chart 1. (Benz)imidazole derived Hg(II)– and Ag(I)–NHC complexes.

molecules as they proved to be less toxic and more effective chemotherapeutic agents.[16] Moreover, these complexes can be applied to the development of tools for biotechnology and biochemistry. Interactions of Ag(I)–NHC complexes with bacterial cell walls and the related biochemistry seem to be of more relevance. In order to find efficient DNA binding agents and to understand the mode of coordination, we prepared and characterized a series of new nitrile-functionalized benzimidazol-2-ylidines and their Ag(I) and Hg(II) complexes. NHC precursors and Ag(I) complexes were screened for their *in vitro* DNA binding activity using different spectral and analytical methods.

Experimental

Reagents and Instruments

All the chemicals used were of reagent grade; solvents were dried and distilled before use according to standard procedures. Benzimidazole, 2-bromomethylbenzonitrile, 3-bromomethylbenzonitrile, *ortho*-dibromomethylxylene, benzyl bromide, *n*-butyl bromide, potassium hexafluorophosphate, silver oxide and mercury acetate were purchased from Sigma-Aldrich and used as received. 1-Benzyl benzimidazole and 1-methylbenzonitrile benzimidazole were prepared according to the literature[17] method with slight modifications. For X-ray single-crystal structure analysis, a Bruker SMART APEX2-2009 CCD area-detector diffractometer was used for data collection. a SAINT Bruker-2009 for cell refinement and SAINT for data reduction, and SHELXTL (Sheldrick, 2008) was used to solve structures.[18] Calculations, structure refinement, molecular graphics and material for publication were performed using the SHELXTL and PLATON (Spek, 2009) software packages.[18] Structures were solved by direct methods and refined by full-matrix least-squares against F^2. FT-IR spectra of compounds were recorded in potassium bromide disks using a PerkinElmer 2000 system spectrometer in the range 4000–400 cm^{-1}. ^1H and ^{13}C NMR spectra were obtained at room temperature on a Bruker 500 MHz Ascend spectrometer in DMSO-d_6 or CD_3CN-d_3 using tetramethylsilane as an internal reference. Melting points were assessed using a Stuart Scientific SMP-1 (UK) instrument. All reported compounds were analyzed for carbon, hydrogen and nitrogen by CHN microanalyses using a PerkinElmer 2400 LS Series CHN/S analyser. Electronic spectra were recorded on a PerkinElmer Lambda 35 spectrometer in the range 1000–200 nm. Molar conductivity measurements were made on a Eutech Instruments CON 510 conductivity meter.

Synthesis of Benzimidazolium Salts

Synthesis of 1-(2-cyanobenzyl)-3-benzyl-3 H-benzimidazol-1-ium hexafluorophosphate (**3**)

A mixture of 2-bromomethyl benzonitrile (0.196 g, 1 mmol) and 1-benzylbenzimidazole (0.208 g, 1 mmol) were stirred in acetonitrile (30 ml) at 100 °C for 48 h. Solvent was removed under reduced pressure, and the product was then washed with diethyl ether (3 × 3 ml). The bromide salt **2** thus obtained was recrystallized from acetonitrile–diethyl ether (1:10 v/v). Salt **2** was directly converted into its dihexafluorophosphate counterpart by metathesis reaction using KPF_6 (0.276 g, 1.5 mmol) in methanol (20 ml). The resultant mixture was stirred for 3 h and was to stand overnight. The pale-green precipitate was filtered under reduced pressure, washed with distilled water (3 × 5 ml) to remove unreacted KPF_6, and air dried. Yield 82.67%; m.p. 110–111 °C. ^1H NMR (500 MHz, d_6-DMSO): δ 5.85 (2 H, s, CH_2-benzyl), 6.08 (2 H, s, CH_2-benzonitrile), 7.40 (3 H, m, 2-CH_{Benzyl}), 7.55 (3 H, m, 3-CH_{Benzyl}), 7.70 (3 H, m, $CH_{Benzimidazole}$), 7.79 (1 H, t, $CH_{Benzimidazole}$, J = 7.8 Hz), 7.90 (1 H, m, 4-$CH_{Benzonitrile}$), 8.0 (2 H, m, 5-$CH_{Benzonitrile}$), 10.04 (1 H, s, benzimidazolium 2-CH). $^{13}C\{^1H\}$NMR (125 MHz, d_6-DMSO): δ 48.60 (CH_2-benzyl), 50.09 (CH_2-benzonitrile), 110.89 (C≡N-nitrile), 113.81, 126.94, 128.75, 133.73, 134.02, (Ar-C_{Benzyl}), 114.18, 127.07, 128.96, 130.96, 133.84, (Ar-$C_{Benzonitrile}$), 116.95, 128.31, 129.14, 129.59, 131.35, 136.91 (Ar-$C_{Benzimidazole}$), 143.49 (benzimidazolium C2′). FT-IR (KBr disc) cm^{-1}: 1602 ν(C≡N, benzimidazole), 2224 ν(C≡N, benzonitrile), 2964, 3033 ν(C-H, aliphatic and aromatic). UV–visible (DMF, nm): 270.1 (π–π^*) and 313.3 (n–π^*). Molar conductance: 16.76 S cm^2 mol^{-1}. Further, molar conductance and ^1H, ^{13}C NMR, FT-IR, UV-visible spectral data of salt **2** has no or negligible changes compared to salt **3**.

Synthesis of 1-(2-cyanobenzyl)-3-butyl-3 H-benzimidazol-1-ium hexafluorophosphate (**5**)

A mixture of 1-methylbenzonitrile benzimidazole (0.233 g, 1 mmol) and *n*-butyl bromide (0.137 g, 1 mmol) was stirred in

acetonitrile (30 ml) at 100 °C for 48 h. Solvent was removed under reduced pressure and the product was washed with diethyl ether (3 × 3 ml). The bromide salt thus obtained was recrystallized from acetonitrile/diethyl ether (1:10 v/v). The bromide salt was directly converted into its dihexafluorophosphate counterpart by metathesis reaction using KPF_6 (0.276 g, 1.5 mmol) in methanol (20 ml). The resultant mixture was stirred for 4 h and was left to stand overnight. The pale-green solid was filtered under reduced pressure, washed with distilled water (3 × 5 ml) to remove unreacted KPF_6, and air dried. Yield 89.02%; m.p. 122 °C. ^{1}H NMR (500 MHz, d_6-DMSO): δ 0.95 (3 H, t, CH_3-butyl, J = 7.5 Hz), 1.40 (2 H, m, CH_2-butyl), 1.90 (2 H, m, CH_2-butyl), 4.60 (2 H, t, CH_2-butyl, J = 7.3 Hz), 6.03 (2 H, s, CH_2-benzonitrile), 7.50 (1 H, d, 2-CH_{Benzyl}, J = 8 Hz), 7.70 (4 H, m, 3-CH_{Benzyl}), 7.90 (1 H, d, 4-CH_{Benzyl}, J = 8 Hz), 8.00 (1 H, d, $CH_{Benzimidazole}$, J = 7.5 Hz), 8.20 (1 H, d, $CH_{Benzimidazole}$, J = 8 Hz), 9.88 (1 H, s, benzimidazolium 2-CH). ^{13}C{^{1}H} NMR (125 MHz, d_6-DMSO): δ 13.35 (CH_3-butyl), 19.02 (CH_2-butyl), 30.53 (CH_2-butyl), 46.67 (N-CH_2-butyl), 48.48 (CH_2-benzonitrile), 110.84 (C ≡ N, nitrile), 113.62, 126.82, 129.11, 131.14, 133.99, (Ar-C, benzonitrile) 116.89, 126.98, 129.58, 131.25, 133.84, 136.9 (Ar-C, benzimidazole), 143.16 (benzimidazolium–C2). FT-IR (KBr disc) cm^{-1}: 1602 ν(C N, benzimidazole), 2225 ν(C ≡ N, benzonitrile), 2962, 3043 ν(C-H, aliphatic and aromatic). UV–visible (DMF, nm): 275.5 (π–π*) and 317.1 (n–π*). Molar conductance: 12.52 S cm^2 mol^{-1}. Further, molar conductance and ^{1}H, ^{13}C NMR, FT-IR, UV–visible spectral data of bromide salt has no or negligible changes compared to salt **5**.

Synthesis of 1-(3-cyanobenzyl)-3-benzyl-3 H-benzimidazol-1-ium hexafluorophosphate (**7**)

This compound was prepared in a manner analogous to that for **3**, only with 3-bromomethyl benzonitrile (0.196 g, 1 mmol) instead of 2-bromomethyl benzonitrile. Yield 78.8%: m.p. 115 °C. ^{1}H NMR (500 MHz, d_6-DMSO): δ 5.81 (2 H, s, CH_2-benzyl), 5.87 (2 H, s, CH_2-benzonitrile), 7.45 (3 H, m, 2-CH_{Benzyl}), 7.55 (2 H, t, 3-CH_{Benzyl}, J = 7.3 Hz), 7.65 (3 H, m, $CH_{Benzimidazole}$), 7.90 (2 H, t, $CH_{Benzimidazole}$, J = 8.0 Hz), 7.90 (2 H, d, $CH_{Benzonitrile}$, J = 7.5 Hz), 10.05 (1 H, s, benzimidazolium 2-CH). ^{13}C{^{1}H}NMR (125 MHz, d_6-DMSO): δ 49.62 (CH_2-benzyl), 50.63 (CH_2-benzonitrile), 112.41 (C ≡ N, nitrile) 127.35, 129.26, 131.62, 133.00 (Ar-C, benzonitrile), 114.36, 127.40, 129.48, 131.52, 133.75 (Ar-C, benzyl), 118.87, 128.84, 130.70, 132.50, 134.27, 135.27 (Ar-C, benzimidazole), 143.55 (benzimidazolium–C2). FT-IR (KBr disc) cm^{-1}: 1605 ν(C N, benzimidazole), 2229 ν(C ≡ N, benzonitrile), 2967, 3032 ν(C-H, aliphatic and aromatic). UV–visible (DMF, nm): 249.6 (π–π*) and 285.2 (n–π*). Molar conductance: 12.9 S cm^2 mol^{-1}. Further, molar conductance and ^{1}H, ^{13}C NMR, FT-IR, UV–visible spectral data of bromide salt **6** had no or negligible changes compared to salt **7**.

Synthesis of 1,2-bis-(3-cyanobenzyl-3 H-benzimidazolium-1-ylmethyl)benzene bis-(hexafluorophosphate) (**9**)

This compound was prepared in a manner analogous to that for **3**, only with 1,2-bis-(3 *H*-benzimidazole-1-ylmethyl)benzene (0.338 g, 1 mmol) and 3-bromomethyl benzonitrile (0.392 g, 2 mmol) instead of 1-benzyl benzimidazole and 2-bromomethyl benzonitrile, respectively. Yield 80.31%; m.p. 145–146 °C. ^{1}H NMR (500 MHz, d_6-DMSO): δ 5.86 (4 H, s, CH_2-benzyl), 6.02 (4 H, s, CH_2-benzonitrile), 7.30 (4 H, m, 3-CH_{Xylyl}), 7.45 (2 H, m, 4-CH_{Xylyl}), 7.70 (6 H, m, $CH_{Benzimidazole}$), 7.90 (6 H, m, $CH_{Benzimidazole}$), 8.00 (2 H, t, $CH_{Benzonitrile}$, J = 8.50 Hz), 9.89 (2 H, s, benzimidazolium 2-CH). ^{13}C{^{1}H}NMR (125 MHz, d_6-DMSO): δ 47.72 (CH_2-benzyl), 49.20 (CH_2-benzonitrile), 111.87, 113.93 (C ≡ N, nitrile), 118.38, 126.92, 130.17, 131.79 (Ar-C, benzonitrile), 127.14, 129.45, 131.92, 135.36 (Ar-C, benzimidazole), 128.86, 132.49, 133.22, (Ar-C, xylene), 143.29 (benzimidazolium–C2). FT-IR (KBr disc) cm^{-1}: 1612 ν(C N, benzimidazole), 2224 ν(C ≡ N, benzonitrile), 2964, 3099 ν(C-H, aliphatic and aromatic). UV–visible (DMF, nm): 292.7 (π–π*) and 315.8 (n–π*). Molar conductance: 37.8 S cm^2 mol^{-1}. Further, molar conductance and ^{1}H, ^{13}C NMR, FT-IR, UV–visible spectral data of bromide salt had no or negligible changes compared to salt **9**.

2.3. Synthesis of NHC Complexes

Synthesis of 1-(2-cyanobenzyl)-3-benzyl-3 H-benzimidazol-1-ium silver(I) hexafluorophosphate (**10**)

A suspension of silver oxide (0.126 g , 0.055 mmol) and **3** (0.469 g, 1 mmol) in methanol (30 ml) was stirred in the absence of light at 50–60 °C for 24 h, after which the mixture was filtered through a pad of celite to remove the unreacted silver oxide. Filtrate was evaporated to dryness under reduced pressure to afford the product as an off-white light-sensitive solid. The complex thus obtained was recrystallized by repeated precipitation in methanol and diethyl ether solution (1:10 v/v). Yield 70.86%; m.p. 278–279 °C. ^{1}H NMR (500 MHz, d_3-CD_3CN): δ 5.59 (4 H, s, CH_2-benzyl), 5.77 (4 H, s, CH_2-benzonitrile), 7.15 (1 H, d, CH_{Benzyl}, J = 8 Hz), 7.40 (2 H, m, $CH_{Benzimidazole}$), 7.55 (2 H, m, $CH_{Benzonitrile}$). ^{13}C{^{1}H}NMR (125 MHz, d_3-CD_3CN): δ 49.49 (CH_2-benzyl), 50.98 (CH_2-benzonitrile), 111.76, 115.02 (C ≡ N, nitrile), 127.98, 130.51, 131.82 (Ar-C,benzonitrile), 129.67, 134.91, 137.71 (Ar-C, benzimidazole), 179.41 (Ag– benzimidazolium C2). FT-IR (KBr disc) cm^{-1}: 1638 ν(C N, benzimidazole), 2224 ν(C ≡ N, benzonitrile), 2923, 3022 ν(C-H, aliphatic and aromatic). UV–visible (DMF, nm): 273.3 (π–π*) and 261.0 (n–π*). Molar conductance: 15.2 S cm^2 mol^{-1}. Anal. Calcd for $C_{44}H_{34}N_6Ag_1F_6P$: C 58.7, H 3.8, N 9.3 %. Found: C 58.2, H 3.1, N 9.6%.

Synthesis of 1-(2-cyanobenzyl)-3-butyl-3 H-benzimidazol-1-ium silver(I) hexafluorophosphate (**11**)

This compound was prepared in a manner analogous to that for **10**, only with **5** (0.435 g, 1 mmol) instead of **3**. Yield 68.56 ; m.p. 165–166 °C. ^{1}H NMR (500 MHz, d_3-CD_3CN): δ 0.85 (3 H, t, CH_3-butyl, J = 7.3 Hz), 1.30 (2 H, m, CH_2-butyl), 1.80 (2 H, m, CH_2-butyl), 4.50 (2 H, t, CH_2-butyl, J = 7.3 Hz), 5.98 (2 H, s, CH_2-benzonitrile), 7.05 (1 H, d, $CH_{Benzimidazole}$, J = 7.8 Hz), 7.45 (3 H, m, $CH_{Benzimidazole}$), 7.62 (2 H, m, $CH_{Benzonitrile}$), 7.90 (2 H, t, $CH_{Benzonitrile}$, J = 7.5 Hz). ^{13}C{^{1}H}NMR (125 MHz, d_3-CD_3CN): δ 14.37 (CH_3-butyl), 20.29 (CH_2-butyl), 32.91 (CH_2-butyl), 49.57 (CH_2-butyl), 51.118 (CH_2-benzonitrile), 111.34 (C ≡ N, nitrile), 112.97, 113.18, 125.16, 128.65, 134.25 (Ar-C, benzonitrile), 117.99, 129.71, 134.46, 134.57 (Ar-C benzimidazole), 180.37 (benzimidazole–C2–Ag). FT-IR (KBr disc) cm^{-1}: 1638 ν(C N, benzimidazole), 2224 ν(C ≡ N, benzonitrile), 2965, 3118 ν(C-H, aliphatic and aromatic). UV–visible (DMF, nm): 287.7 (π–π*) and 267.0 (n–π*). Molar conductance: 17.90 S cm^2 mol^{-1}. Anal. Calcd for $C_{38}H_{38}N_6Ag_1F_6P$: C 54.9, H 4.6, N 10.1%. Found: C 55.4, H 4.9, N 9.7%.

Synthesis of 1-(3-cyanobenzyl)-3-benzyl-3 H-benzimidazol-1-ium silver(I) hexafluorophosphate (**12**)

This compound was prepared in a manner analogous to that for **10**, only with **7** (0.469 g, 1 mmol) instead of **3**. Yield 71.56%, m.p. 214 °C. ^{1}H NMR (500 MHz, d_6-DMSO): δ 5.77 (2 H, s, CH_2-benzyl), 5.82 (2 H, s, CH_2-benzonitrile), 7.30 (3 H, m, CH_{Benzyl}), 7.36 (2 H, d, CH_{Benzyl}, J = 7.00 Hz), 7.41 (2 H, m, $CH_{Benzimidazole}$), 7.55 (1 H, d,

$CH_{Benzimidazole}$, $J = 8.00$ Hz), 7.64 (1 H, d, $CH_{Benzimidazole}$, $J = 8.00$ Hz), 7.72 (2 H, m, $CH_{Benzonitrile}$), 7.76 (2 H, m, $CH_{Benzonitrile}$). $^{13}C\{^1H\}$NMR (125 MHz, d_6-DMSO): δ 49.51 (CH_2-benzyl), 50.41 (CH_2-benzonitrile), 113.36 (C ≡ N, benzonitrile), 126.10, 128.01, 130.32, 132.05 (Ar-C, benzonitrile), 126.15, 128.58, 128.94, 134.30 (Ar-C, benzimidazole), 164.92 (Ag–benzimidazolium–C2). FTIR (KBr disc) cm^{-1}: 1605 ν(C N, benzimidazole), 2230 ν(C ≡ N, benzonitrile), 2924, 3062 ν(C-H, aliphatic and aromatic). UV–visible (DMF, nm): 257.2 (π–π*) and 261.9 (n–π*). Molar conductance: 13.55 S cm^2 mol^{-1}. Anal. Calcd for $C_{44}H_{34}N_6Ag_1F_6P$: C 58.7, H 3.8, N 9.3%. Found: C 59.0, H 3.7, N 9.8%.

Synthesis of 1-(2-cyanobenzyl)-3-benzyl-3 H-benzimidazol-1-ium mercury(II) bis-hexafluorophosphate (**13**)

Mercury acetate (0.159 g, 0.5 mmol) was added to a solution of **3** (0.469 g, 1 mmol) in methanol (20 ml). The mixture was heated at 80–90 °C for 24 h, after which the solvent was removed under reduced pressure to give a pale-yellow powder. The complex thus obtained was collected and recrystallized by repeated precipitation from methanol and diethyl ether mixture (1:10 v/v) to gave the complex as a white powder. Yield 70.14%, m.p. 255–256 °C. ^{1}H NMR (500 MHz, d_3-CD_3CN): δ 5.98 (4 H, s, CH_2-benzyl), 6.24 (4 H, s, CH_2-benzonitrile), 6.85 (1 H, d, CH_{Benzyl}, $J = 8.0$ Hz), 7.37 (8 H, m, CH_{Benzyl}), 7.50 (4 H, d, $CH_{Benzimidazole}$, $J = 8.50$ Hz), 7.55 (6 H, m, $CH_{Benzimidazole}$), 7.70 (2 H, d, $CH_{Benzonitrile}$, $J = 8.0$ Hz), 7.79 (2 H, s, $CH_{Benzonitrile}$). $^{13}C\{^1H\}$NMR (125 MHz, CD_3CN-d_3): δ 51. 8 (CH_2-benzyl), 52.08 (CH_2-benzonitrile), 110.01, 113.51 (C ≡ N, nitrile), 117.11, 126.30, 127.72, 128.43, 133.62 (Ar-C, benzonitrile), 126.40, 128.67, 128.79, 133.51, (Ar-C, benzimidazole), 176.51 (Hg–benzimidazolium C2). FT-IR (KBr disc) cm^{-1}: 1569 ν(C&dtbond;N, benzimidazole), 2225 ν(C ≡ N, benzonitrile), 2925, 3069 ν(C-H, aliphatic and aromatic). UV–visible (DMF, nm): 278.2 (π–π*) and 290.7 (n–π*). Molar conductance: 31.4 S cm^2 mol^{-1}. Anal. Calcd for $C_{44}H_{34}N_6Hg_1F_{12}P_2$: C 46.5, H 3.0, N 7.4%. Found: C 46.0, H 3.7, N 7.8%.

Synthesis of 1-(2-cyanobenzyl)-3-butyl-3 H-benzimidazol-1-ium mercury(II) bis-hexafluorophosphate (**14**)

This compound was prepared in a manner analogous to that for **13**, only with **5** (0.435 g, 1 mmol) instead of **3**. Yield 56.07%, m.p. 182 °C. ^{1}H NMR (500 MHz, d_3-CD_3CN): δ 1.00 (3 H, t, CH_3-butyl, $J = 7.3$ Hz), 1.14 (2 H, m, CH_2-butyl), 1.97 (2 H, m, CH_2-butyl), 4.65 (2 H, t, CH_2-butyl, $J = 7.8$ Hz), 6.04 (2 H, s, CH_2-benzonitrile), 7.39 (2 H, m, CH_{Benzyl}), 7.52 (2 H, t, CH_{Benzyl}, $J = 7.5$ Hz), 7.60 (4 H, t, $CH_{Benzimidazole}$, $J = 8.3$ Hz), 7.95 (2 H, d, $CH_{Benzonitrile}$, $J = 7.0$ Hz). $^{13}C\{^1H\}$NMR (125 MHz, CD_3CN-d_3): δ 13.27 (CH_3-butyl), 19.95 (CH_2-butyl), 32.33 (CH_2-butyl), 49.79 (N-CH_2-butyl), 65.65 (CH_2-benzonitrile), 113.66, 113.87 (C ≡ N, nitrile), 127.13, 133.68, 134.33 (Ar-C, benzonitrile), 128.38, 129.80, 134.15, 137.54 (Ar-C, benzimidazole), 176.20 (Hg–benzimidazole C2). FT-IR (KBr disc) cm^{-1}: 1588 ν(C N, benzimidazole), 2224 ν(C ≡ N, benzonitrile), 2963, 3108 ν(C-H, aliphatic and aromatic). UV–visible (DMF, nm): 292.2 (π–π*) and 281.4 (n–π*). Molar conductance: 35.19 S cm^2 mol^{-1}. Anal. Calcd for $C_{38}H_{38}N_6Hg_1F_{12}P_2$: C 42.7, H 3.6, N 7.9%. Found: C 42.4, H 3.9, N 7.7%.

Synthesis of 1-(3-cyanobenzyl)-3-benzyl-3 H-benzimidazol-1-ium mercury(II) bis-hexafluorophosphate (**15**)

This compound was prepared in a manner analogous to that for **13**, only with **7** (0.469 g, 1 mmol) instead of **3**. Yield 58.02%, m.p. 252–253 °C. ^{1}H NMR (500 MHz, d_3-CD_3CN): δ 5.97 (2 H, s, CH_2-benzyl), 6.00 (2 H, s, CH_2-benzonitrile), 7.37 (4 H, m, CH_{Benzyl}), 7.51 (5 H, m, CH_{Benzyl}), 7.60 (2 H, t, $CH_{Benzimidazole}$, $J = 7.8$ Hz), 7.73 (2 H, m, $CH_{Benzimidazole}$), 7.83 (2 H, m, $CH_{Benzonitrile}$), 7.93 (1 H, s, $CH_{Benzonitrile}$). $^{13}C\{^1H\}$NMR (125 MHz, d_3-CD_3CN): δ 50.78 (CH_2-benzyl), 51.88 (CH_2-benzonitrile), 111.74, 113.52 (C ≡ N, benzonitrile), 118.44, 126.25, 128.75, 129.94, 132.15, 132.54, 132.70, 136.28 (Ar-C, benzonitrile), 127.68, 131.25, 132.65, 134.60 (Ar-C, benzimidazole), 174.01 (Hg–benzimidazolium C2). FTIR (KBr disc) cm^{-1}: 1574 ν(C N, benzimidazole), 2225 ν(C ≡ N, benzonitrile), 2925, 3069 ν(C-H, aliphatic and aromatic). UV–visible (DMF, nm): 280.8 (π–π*) and 293.0 (n–π*). Molar conductance: 30.7 S cm^2 mol^{-1}. Anal. Calcd for $C_{44}H_{34}N_6Hg_1F_{12}P_2$: C 46.5, H 3.0, N 7.4%. Found: C 46.6, H 3.3, N 7.7%.

Synthesis of 1-(2-((1 H-benzimidazol-1-yl)methyl)benzyl)-1 *H*-benzimidazole disilver(I) bis-hexafluorophosphate (**16**)

This compound was prepared in a manner analogous to that for **10**, only with **9** (0.862 g, 1 mmol) instead of **3**. Yield 70.6%; m.p. 251–252 °C. ^{1}H NMR (500 MHz, d_6-DMSO): δ 5.49 (2 H, s, CH_2-benzyl), 5.67 (2 H, s, CH_2-benzonitrile), 7.16 (3 H, m, 3-CH_{Xylyl}), 7.40 (3 H, m, 4-CH_{Xylyl}), 7.66 (3 H, m, $CH_{Benzimidazole}$), 7.69 (1 H, s, $CH_{Benzimidazole}$), 7.77 (1 H, m, $CH_{Benzonitrile}$). $^{13}C\{^1H\}$NMR (125 MHz, d_6-DMSO): δ 50.96 (CH_2-benzyl), 51.66 (CH_2-benzonitrile), 111.71, 112.25 (C ≡ N, nitrile), 118.40, 124.22, 126.49, 129.02, (Ar-C_{Xylyl}) 124.32, 127.98, 130.81, 133.48, 134.72 (Ar-$C_{Benzimidazole}$), 126.85, 136.49, 137.85 (Ar-$C_{Benzonitrile}$), 171.48 (Ag–benzimidazolium 2C). FTIR (KBr disc) cm^{-1}: 1618 ν(C N, benzimidazole), 2229 ν(C ≡ N, nitrile), 2917, 3033 ν(C-H, aliphatic and aromatic). UV–visible (DMF, nm): 256.61 (π–π*) and 261.28 (n–π*). Molar conductance: 28.61 S cm^2 mol^{-1}. Anal. Calcd for $C_{76}H_{56}N_{12}Ag_2F_{12}P_2$: C 55.6, H 3.4, N 10.2%. Found: C 56.8, H 3.7, N 10.7%.

Synthesis of 1-(2-((1 H-benzimidazol-1-yl)methyl)benzyl)-1 *H*-benzimidazole dimercury(II) tetra-hexafluorophosphate (**17**)

This compound was prepared in a manner analogous to that for **13**, only with **9** (0.862 g, 1 mmol) instead of **3**. Yield 71.18%; m.p. 256–257 °C. ^{1}H NMR (500 MHz, d_6-DMSO): δ 6.51 (2 H, s, CH_2-benzyl), 6.58 (2 H, s, CH_2-benzonitrile), 7.92 (4 H, m, CH_{Xyly}), 8.24 (7 H, m, CH_{Xylyl}), 8.35 (1 H, m, $CH_{Benzimidazole}$, $J = 8.00$ Hz), 8.45 (1 H, m, $CH_{Benzonitrile}$, $J = 8.00$ Hz). $^{13}C\{^1H\}$NMR (125 MHz, d_6-DMSO): δ 49.40 (CH_2-benzyl), 51.50 (CH_2-benzonitrile), 112.59, 113.21 (C ≡ N, nitrile), 117.89, 126.96, 129.53, 131.22 (Ar-C_{Xylyl}), 127.69, 129.69, 130.08, 132.32, 135.27 (Ar-$C_{Benzimidazole}$), 129.87, 130.69, 131.85, 132.97, 133.78, (Ar-$C_{Benzonitrile}$), 176.49 (Hg–benzimidazolium 2C). FTIR (KBr disc) cm^{-1}: 1578 ν(C N, benzimidazole), 2232 ν(C ≡ N, benzonitrile), 2965, 3030 ν(C-H, aliphatic and aromatic). UV–visible (DMF, nm): 265.11 (π–π*) and 293.8 (n–π*). Molar conductance: 143.25 S cm^2 mol^{-1}. Anal. Calcd for $C_{76}H_{56}N_{12}Hg_2F_{12}P_2$: C 49.9, H 3.1, N 9.2%. Found: C 50.6, H 3.6, N 9.8%.

Methodology for Nuclease Activity

Supercoiled plasmid DNA pUC19 was used for DNA cleavage experiments using agarose gel electrophoresis. Plasmid DNA (pDNA) from the overnight-grown *E. coli* cells were isolated using Wizard® *Plus* SV Minipreps DNA purification system (Promega, Madison, WI, USA). pDNA (200 ng) in 5 mM Tris–HCl/50 mM NaCl buffer (pH 7.2) was treated with ligands and its Ag complexes (150 mM) with or without H_2O_2 (100 mM) for 2 h at 37 °C. After incubation, 20 μl of the reaction mixture was loaded on to 1% agarose gel prepared with 1× TAE (Tris–acetic acid–ethylenediaminetetraacetic acid (EDTA)) buffer solution and electrophoresed

for 50 min at 70 mV in a gel electrophoresis apparatus (Bio-Rad, California, USA) with 0.5× TAE buffer (pH 8.3). The gel was then stained with 1 μg ml^{-1} ethidium bromide and visualized under UV light using a gel documentation system (FluorChem HD2, Cell Biosciences) and photographed. The nucleating ability of the synthesized benzimidazolium salts/Ag complexes was determined by its efficiency in cleaving the supercoiled (SC) plasmid DNA into open circular (OC) or nicked circular (NC) forms.

Methodology for DNA Binding Activity

Isolation of genomic DNA

Escherichia coli genomic DNA (gDNA) was utilized for the benzimidazolium salts/Ag complexes DNA binding studies. *E. coli* JM109 strain was grown overnight and the gDNA was extracted using commercially available DNA isolation kit (DNeasy®, QIAGEN, Hilden, Germany).

DNA binding analysis using electronic spectral method

The concentration of gDNA per nucleotide [*C*(p)] was measured by using its known extinction coefficient at 260 nm (6600 M^{-1} cm^{-1}). The absorbance at 260 nm (A_{260}) and at 280 nm (A_{280}) for DNA was measured to check its purity, and was found to be satisfactorily free from protein. Buffer (5 mM tris(hydroxymethyl) aminomethane, pH 7.2, 50 mM EDTA] was used. In absorption studies the complex was dissolved in DMF to obtain the desired concentration. Spectroscopic titrations were carried out by adding increasing amounts (20–100 μl) of DNA to a solution of the complex at a fixed concentration contained in a quartz cell. The UV–visible spectra were recorded after equilibration at 27 °C for 10 min after each addition. The intrinsic binding constant K_b was determined from the plot of [DNA]/($\varepsilon_a - \varepsilon_f$) vs. [DNA] according to equation (1):

$$[\mathrm{DNA}]/(\varepsilon_a - \varepsilon_f) = [\mathrm{DNA}]/(\varepsilon_b - \varepsilon_f) + 1/[K_b(\varepsilon_b - \varepsilon_f)] \qquad (1)$$

where [DNA] is the concentration of DNA in base pairs, the apparent absorption coefficients ε_a, ε_f and ε_b correspond to A_{obs}/[complex], extinction coefficient for the free complex and the extinction coefficient of the complex in the totally bound form, respectively. The data were fitted to equation (1), with a slope equal to 1/($\varepsilon_b - \varepsilon_f$) and *y*-intercept equal to 1/[*K*b($\varepsilon_b - \varepsilon_f$)] and K_b was obtained from the ratio of the slope to the intercept.

DNA binding analysis using viscosity measurements

Viscosity measurements were carried out using an Oswald microviscometer, maintained at constant temperature (29 °C) in a thermostat. DNA concentration was kept constant in all samples, but the complex concentration was increased each time (from 200 to 1000 μM). Mixing of the solution was achieved by bubbling nitrogen gas through the viscometer. The mixture was left for 10 min at 29 °C after addition of each aliquot of complex. The flow time was measured with a digital stopwatch. The experiment was repeated in triplicate to obtain the concurrent values. Data are presented as $(\eta/\eta_0)^{1/3}$ vs. the ratio [complex]/[DNA], where η and η_0 are the specific viscosity of DNA in the presence and in absence of the complex, respectively. The values of η and η_0 were calculated using equation (2):

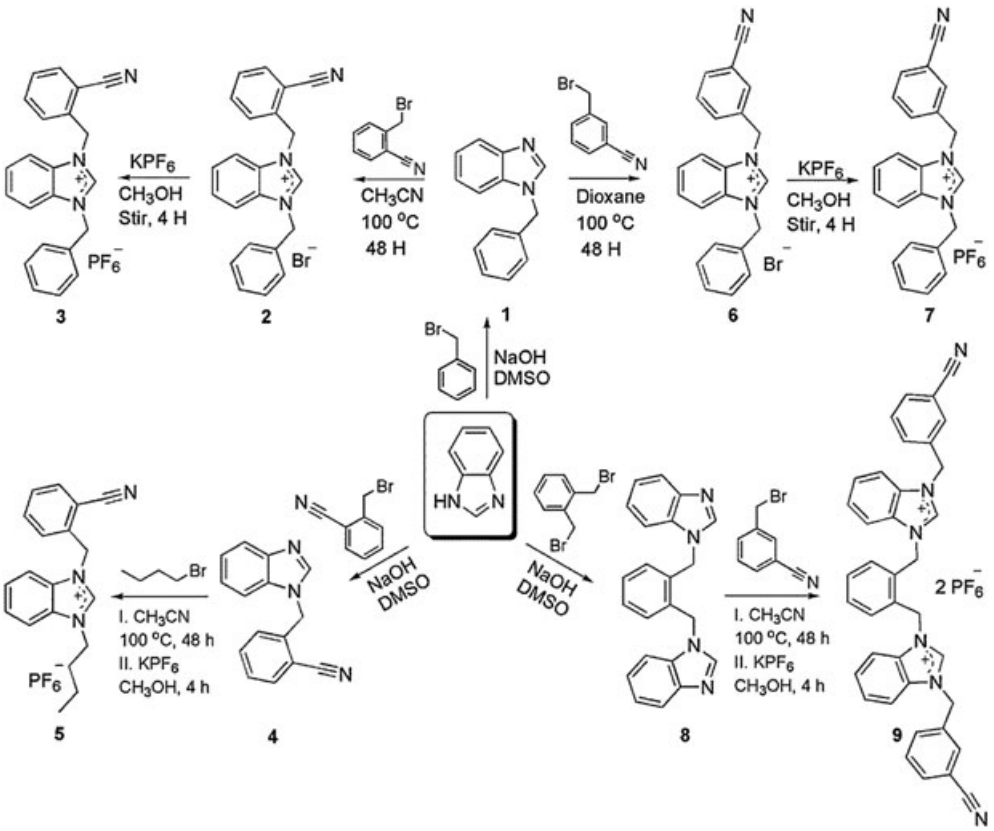

Scheme 1. Synthetic route to the preparation of benzimidazolium salts **2–9**.

$$\eta = (t - t_b)/t_b \quad (2)$$

where t_b is the observed flow time of DNA containing solution and t is the flow time of buffer alone. Relative viscosities for DNA were calculated from the relation η/η_o.

Results and Discussion

Syntheses

1-(2-nitrilebenzyl) benzimidazole was prepared according to the similar method reported for the preparation of 1-benzyl benzimidazole and *ortho*-xylyl-bis-benzimidazole with slight modifications.[17] A mixture of benzimidazole and NaOH (1:2) was stirred in THF at 70 °C for 3 h. 2-Bromomethylbenzonitrile (1 equiv.) in THF was added dropwise to the mixture and further stirred under the same conditions for 24 h. The light-brown solid was obtained after solvent removal using a rotary evaporator, washed with distilled water to remove the unreacted NaOH and air dried.

The synthetic route for both the 2-nitrile and 3-nitrile-substituted benzimidazolium salts is shown in Scheme 1. 2-Nitrile-substituted benzimidazolium bromide salts **2** and **4** were prepared by the reaction of 1-benzyl benzimidazole and 1-methylbenzonitrile benzimidazole with 2-bromomethyl benzonitrile and butyl bromide, respectively, in acetonitrile at refluxing conditions for 48 h. Similarly, 3-nitrile-substituted bromide salts were prepared by the reaction of 3-bromomethylbenzonitrile with 1-benzylbenzimidazole or 1,2-bis-(3 *H*-benzimidazole-1-ylmethyl)benzene in acetonitrile under reflux conditions. Hexafluorophosphate salts of the NHC precursors are found to be considerably more stable than the corresponding bromide salts in common organic solvents such as acetonitrile and acetone. Therefore the bromide salts were converted into their hexafluorophosphate counterparts by the salt metathesis reaction using KPF_6 in methanol to afford salts **3**, **5**, **7** and **9** in good yields. These salts are readily soluble in common organic solvents such as acetonitrile, DMF and DMSO, but are insoluble in toluene, methanol and 1,4-dioxane.

Reactions involved in the preparation of mononuclear and binuclear carbene complexes are shown in Schemes 2 and 3, respectively. Ag(I) and Hg(II)–carbene complexes have been prepared by the *in situ* deprotonation method using basic metal sources.[19] Reactions of benzimidazolium salts **3**, **5**, **7** and **9** in acetonitrile at refluxing conditions for 24–36 h with $Ag_2O/Hg(OAc)_2$ yield off-white, light-sensitive Ag(I)–carbene complexes **10**, **11**, **12** and **16**, and Hg(II)–carbene complexes **13**, **14**, **15** and **17**, respectively, in moderately good yields (55.0–70.9%). All the carbene complexes were purified by repeated precipitation in acetonitrile by the addition of diethyl ether. In the case of Ag(I) complexes, the unreacted silver oxide was filtered through a pad of celite. However, in the case of Hg (II) complexes, the excess or residual $Hg(OAc)_2$ was removed by repeated washing with distilled water. Both, Ag(I)– and Hg(II)–carbene complexes are soluble in polar organic solvents such as acetonitrile, DMF and DMSO, but are insoluble in toluene, diethyl ether, benzene and hexane.

NMR Spectral Studies

The NMR spectrum of all the compounds has been analysed in appropriate deuterated solvents over the scan ranges δ 0–16 and 0–200 for ^{1}H and ^{13}C NMR spectral studies, respectively. The ^{1}H NMR spectrum of benzimidazolium salts shows two distinctive singlets in the range δ 5.71–6.02, indicating the

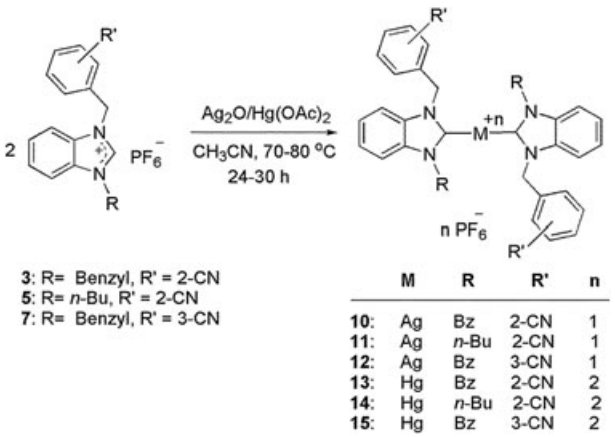

	M	R	R'	n
10:	Ag	Bz	2-CN	1
11:	Ag	*n*-Bu	2-CN	1
12:	Ag	Bz	3-CN	1
13:	Hg	Bz	2-CN	2
14:	Hg	*n*-Bu	2-CN	2
15:	Hg	Bz	3-CN	2

Scheme 2. Synthesis of mononuclear Ag(I)– and Hg(II)–NHC complexes **10–15**.

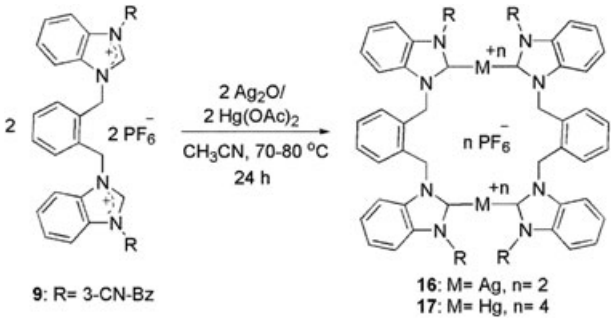

Scheme 3. Synthesis of binuclear Ag(I)– and Hg(II)–NHC complexes **16** and **17**.

presence of benzylic and benzonitrilic protons. The multiplets in the range δ 7.41–8.19 and 1.3–4.2 are due to the resonance of aromatic and aliphatic protons. Spectra also evidenced a characteristic downfield resonance in the range δ 9.87–10.06 corresponding to the NCHN proton, indicating the successful formation of benzimidazolium salts.[20–22] This down-field shift of the NCHN protons is due to their deshielding by two adjacent electronegative nitrogen atoms that withdraw higher electron density from around the benzimidazolium proton compared to other protons. The ^{13}C NMR spectra of the benzimidazolium salts display characteristic downfield resonances in the range δ 143.47–148.15 for the NCN carbon nuclei.[23,24] In addition, spectra also evidenced aromatic, nitrile, benzylic and aliphatic carbon resonances in the range δ 118–138, 111–114, 48–53 and 13–43, respectively.

The successful formation of carbene complexes is indicated by the disappearance of the characteristic acidic 2 *H*-benzimidazolium protons in the ^{1}H NMR spectra of complexes **10–17** via deprotonation. In addition, in the ^{13}C NMR spectra of the complexes, the characteristic carbene carbon (Ag-C and Hg-C) value in the range δ 164–189 is consequently observed. These observations collectively confirm the formation of desired Ag(I)– and Hg(II)–NHC complexes.[25] Apart from this major change, both ^{1}H and ^{13}C NMR spectra of the complexes showed resonances of aromatic, nitrile, benzylic and aliphatic carbon nuclei in the range δ 118–138, 112–114, 49–53 and 12–41, respectively. These values are in agreement with the reported Ag(I)– and Hg(II)–NHC complexes.[26–28]

FT-IR Spectral Studies

Both benzimidazolium salts and their Ag(I)– and Hg(II)–NHC complexes were characterized by FT-IR spectral technique over the range 4000–400 cm^{-1}. IR spectra of the benzimidazolium salts show a strong band at around 1605 cm^{-1} with medium intensity, assigned to the stretching vibrations of the benzimidazole ring C N module.[29] A sharp band of medium intensity was observed at 2225 cm^{-1}, assigned to the stretching vibrations of nitrile component. In addition, spectra also evidenced at the two bands around 2960 and 3030 cm^{-1}, which were assigned to the pure modes of the C-H stretching vibrations. This variation in the range is due to the presence of aliphatic and aromatic C-H modules.[30] However, in the complex spectra, the band due to benzimidazole ring vibrations showed a negative shift, further indicating the formation of C-N module and in turn the desired carbene complexes. Furthermore, a non-ligand band with medium intensity at around 1100 cm^{-1} further confirms its formation. Interestingly, nitrile stretching vibrations remain unaltered in the complex spectra, indicating their presence outside the coordination spear.

UV–visible Spectral Studies

The electronic spectra of salts and complexes were recorded in DMF solution (10^{-3} M concentration) over the range 1000–200 nm. All the benzimidazolium salts show two characteristic bands in the range 255–267 and 290–310 nm assigned to intramolecular $\pi \rightarrow \pi^*$ and $n \rightarrow \pi^*$ transitions originating from the C C, C N and C ≡ N modules.[31] These bands show a negative shift of about 18–21 nm upon complexation with Ag(I) or Hg(II), indicating the formation of a C-N module in the benzimidazole ring. In addition, complex spectra showed a band at around 320 nm and this accounted for the charge transfer transitions. No bands at lesser energy level for d–d transition were observed, as expected.

Molar Conductivity Measurements

The molar conductance value of benzimidazolium salts and complexes was obtained at room temperature in DMF solution at 10^{-3} mol dm^{-3} concentration. The molar conductivity value of benzimidazolium salts **3**, **5**, **7** and their Ag(I)–carbene complexes **10**, **11**, **12** is found to be similar, in the range 13.5–18.5 S cm^2 mol^{-1}, indicating that they are 1:1 electrolytes.[32] However, in the case of benzimidazolium salt **9** and its Ag(I)–carbene complex **16**, and Hg(II)–carbene complexes **13**, **14** and **15**, this value is almost double, indicating that they are 2:2 electrolytes. Finally, a value of 143.25 S cm^2 mol^{-1} was observed in the case of Gg(II)–carbene complex **17**, indicating a 4:4 electrolytic nature. Furthermore, we also tried to deduce the structure of compounds on the basis of their molar conductivity measurements. It is evident from this study that the mononuclear Ag(I)– and Hg(II)–carbene complexes have one and two hexafluorophosphate counterions, respectively, which in turn reflects the formation of a bis-carbene complex. Similarly, complexes **16** and **17** were also found to be bis-carbene analogues containing a bimetallic core.

Single-Crystal X-Ray Diffraction Studies

X-ray-quality crystals of salts **2** and **5** were grown by slow evaporation of a salt solution in acetonitrile 1,4-dioxane at ambient temperature. A perspective view of salts **2** and **5** and their crystal packing are shown in Figs 1–4. The crystal refinement data and selected bond lengths and angles of salts **2** and **5** are tabulated in Tables 1, 2 and 3.

Salt **2** crystallizes in the monoclinic space group *P*2(1)/*c* with one benzimidazolium cation, one bromide anion and one water molecule occupying an asymmetric unit. Each repeating unit of the crystal consists of four benzimidazolium units, four bromide counterions and four water molecules. Planes of both the *N*-substituents on the benzimidazole ring, benzyl and benzonitrile are almost parallel to each other but perpendicular to the plane of the central benzimidazole core. In the salt, the central benzimidazolium ring of the monocation makes dihedral angles of 131.3(2)° and 112.45(19)° with the pendant benzyl and benzonitrile rings, respectively. The internal ring angle, N1–C7–N2, at the carbene centre is found to be 110.8(2)°, which is consistent with earlier reports.[33,34] In the extended structure, benzimidazolium cations and bromides are connected via C-H. . .Br and C-H. . .O hydrogen bonds (2.884 and 3.635 Å), forming a three-dimensional array. Each bromide ion is connected with eight different hydrogen atoms to form the aforementioned hydrogen bonds, and surprisingly, shows a weak interaction with the oxygen atom of the water molecule (Br-O), with a bond distance of 3.112 Å, perpendicular to the *ab* plane.

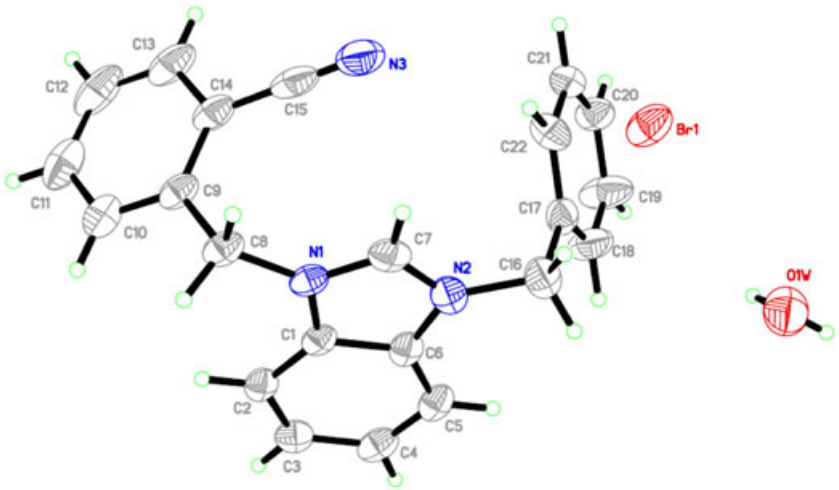

Figure 1. Molecular structure of benzimidazolium salt **2** with displacement ellipsoids drawn at 50 % probability.

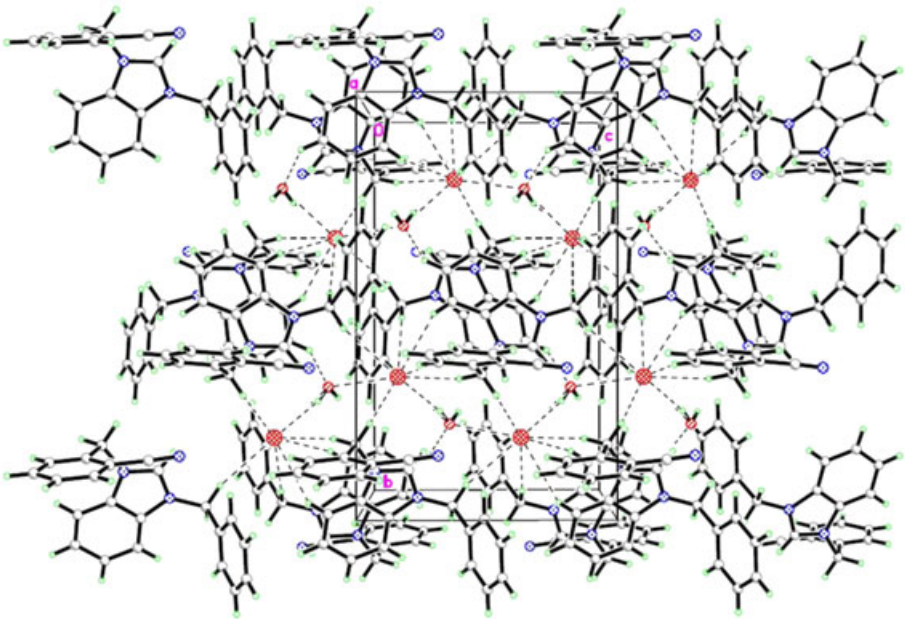

Figure 2. The crystal packing of salt **2**, showing the C-H. . .Br, C-H. . .O and O-H. . .Br hydrogen bonds as dashed lines.

The asymmetric unit of salt **5** contains one benzimidazolium cation and one hexafluorophosphate anion. This salt crystallizes in the monoclinic space group *P*2(1)/*c*. Each repeating unit of the crystal consists of four benzimidazolium units and four hexafluorophosphate counterions. The benzonitrile ring and *n*-butyl chain are inclined at an angle of 113.07(12)° and 113.23 (13)°, respectively, with respect to the central benzimidazolium ring. The internal ring angle, N1–C7–N2, at the carbene centre is 110.33(14)°, which is in agreement with the reported compounds.[33,34] In the extended structure, benzimidazolium cations and hexafluorophosphate anions are connected via C-H. . .F and C-H. . .N≡C hydrogen bonds (2.947 and 2.647 Å), forming a three-dimensional network.

Nuclease Activity of the Benzimidazolium Salts and their Ag Complexes

Gel electrophoresis was used to evaluate the DNA cleavage properties of benzimidazolium salts **3**, **5**, **7** and **9** and the respective Ag(I)–NHC complexes **10**, **11**, **12** and **16**. Agarose gel images indicating the nuclease activity of the compounds in the presence and absence of oxidizing agent H_2O_2 are shown in Figs 5 and 6, respectively. When supercoiled pUC19 plasmid DNA was electrophoresed, the strands migrated along the gel. This supercoiled confirmation (form I) had a faster migration when compared to its closed circular confirmation (form II), which was produced as a result of the cleavage of one of the strands of the double helix. However, when both strands were cleaved a linear confirmation (form III) DNA was formed, which migrated between form I and form II.[35] By analysing the migration of pDNA in the agarose gel, the extent of DNA damage can be evaluated. A control experiment using a mixture of DNA and oxidizing agent, and DNA alone, did not show any significant cleavage.

Among the tested 2-nitrile-substituted compounds, benzimidazolium salt **5** displayed remarkable DNA cleavage activity in the absence of oxidizing agent H_2O_2. Surprisingly, though, its activity was seen to reduce in the presence of H_2O_2. Other tested compounds containing 2-nitrile substitution displayed no

Figure 3. Molecular structure of benzimidazolium salt **5** with displacement ellipsoids drawn at 50 % probability.

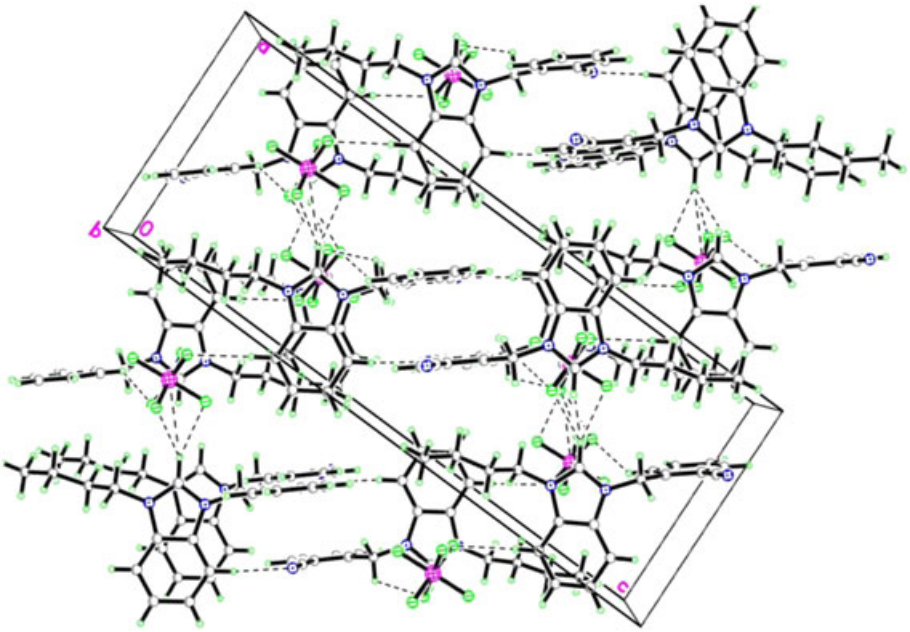

Figure 4. The crystal packing of salt **5**, showing the C-H. . .F and C-H. . .N hydrogen bonds as dashed lines.

obvious visible activity towards the cleavage of DNA into form III, either in the presence or absence of H_2O_2. However, the width of the DNA band became smaller and intense in appearance and showed smearing to a lesser extent, indicating their binding properties rather than cleavage. On the other hand, compounds derived from 3-nitrile-substituted benzimidazolium salts evidenced distinct nuclease activity. Salt **9** and its Ag complex **16** efficiently cleaved supercoiled pDNA form into linear form (form III) in the presence and absence of oxidizing agent. A smear following the band indicates further cleavage of the strands. This infers that further incubation above 2 h could possibly have initiated complete degradation of the pDNA. Perhaps the observed nuclease activity of the salts and complex was due to the hydrolytic cleavage of DNA catalysed by the complex. This could be attributed to the binuclear nature of the complex and the appropriate substitutions on it.

Table 1. Crystal data and structure refinement details for **2** and **5**

	2	**5**
Formula	$C_{22}H_{19}BrN_3$	$C_{19}H_{20}F_6N_3P$
Formula weight	413.31	435.35
Crystal system	Monoclinic	Monoclinic
Space group	*P*2(1)/*c*	*P*2(1)/*c*
Unit cell dimensions		
a (Å)	12.5545(2)	9.52740(10)
b (Å)	15.7849(2)	8.42460(10)
c (Å)	9.6485(2)	24.8761(3)
α (°)	90.00	90.00
β (°)	91.6330(10)	92.4310(10)
γ (°)	90.00	90.00
V (Å^3)	1911.28(6)	1994.87(4)
Z	4	4
Density (calcd) (g cm^{-3})	1.436	1.450
Absorp. coeff. (mm^{-1})	2.164	0.202
F(000)	844	896
Crystal size (mm)	0.45 × 0.31 × 0.25	0.34 × 0.20 × 0.11
Temperature (K)	100(2)	100(2)
Radiation (Å)	Mo *K*α 0.71073	Mo *K*α 0.71073
θ min., max. (°)	1.62, 33.57	2.14, 30.32
Dataset	−19:19, −24:24, −13:14	−13:12, −11:11, −30:35
Tot.; unique data	28753	22074
R (int.)	0.0321	0.0231
N_{ref}, N_{par}	7484, 263	5944, 263
R, wR_2, *S*	0.0835, 0.1416, 1.048	0.0753, 0.1079, 1.010

DNA Binding Activity Using Electronic Spectral Method

The UV–visible spectral technique is the most frequently used method to study the interaction of transition metal complexes with DNA, since these complexes often have abundant spectroscopic properties.[36,37] Normally, DNA binding ability of the complexes is assessed by measuring the effects on their UV spectra in the presence of DNA.[38] UV–visible absorption titration spectra of complexes **10** and **16** are shown in Figs 7 and 8, respectively. Addition of increasing amounts of DNA resulted in a decrease of absorbance for each investigated benzimidazolium salt and complex. With increasing concentration of DNA, the absorption bands of both the benzimidazolium salts and Ag(I) complexes were affected, resulting in a tendency to hypochromism and a remarkable red shift. This can be attributed to the intercalative mode of the binding of tested compounds to the double helix of DNA.[40] This may be due to the presence of benzimidazole or central xylyl cores, which may provide an aromatic unit by which overlapping would occur with the DNA base pairs via an intercalative mode of binding. Change in absorbance at the peak maximum of benzimidazolium salts and their Ag complexes of the most red-shifted band of each compound with increasing concentration of DNA has been monitored for evaluation of the intrinsic binding constant (K_b). The K_b values (Table 4) of the benzimidazolium salts are sufficiently less than the corresponding Ag complexes. Similar observations

Table 2. Selected bond lengths (Å) and angles (°) of **2**

C8–C9	1.521(3)	N1–C7	1.334(4)	N2–C7	1.329(4)
C16–C17	1.514(4)	N1–C8	1.470(3)	N2–C16	1.477(4)
N1–C1	1.392(3)	N2–C6	1.398(3)	N3–C15	1.152(7)
C2–C1–N1	131.7(2)		N1–C8–C9	112.45(19)	
C5–C6–N2	111.3(2)		N2–C7–N1	110.8(2)	
C7–N1–C1	107.9(2)		N2–C16–C17	131.3(2)	
C7–N2–C6	108.2(2)		N3–C15–C14	178.0(4)	

Table 3. Selected bond lengths (Å) and angles (°) of **5**

C8–C9	1.516(2)	N1–C8	1.4610(19)	N2–C16	1.4734(19)
N1–C1	1.336(2)	N2–C1	1.3282(19)	N3–C15	1.148(2)
N1–C2	1.392(2)	N2–C7	1.393(2)		
C1–N1–C8	125.05(14)		C7–N2–C16	126.30(13)	
C1–N1–C2	108.32(13)		N1–C8–C9	113.07(12)	
C1–N2–C7	108.31(13)		N2–C1–N1	110.33(14)	
C1–N2–C16	125.33(14)		N2–C16–C17	113.23(13)	
C2–N1–C8	126.63(13)		N3–C15–C14	178.56(18)	

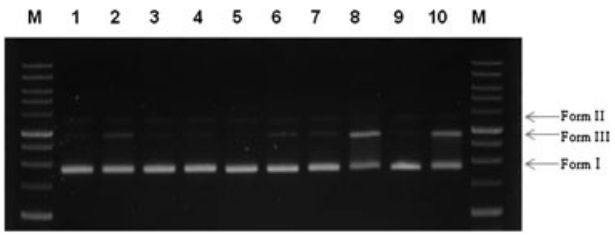

Figure 5. Ethidium bromide stained agarose gel (1%) picture of benzimidazolium salts and their Ag(I) complexes in the presence of oxidizing agent H_2O_2.

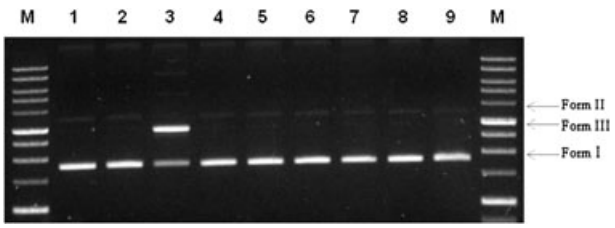

Figure 6. Ethidium bromide stained agarose gel (1%) image of benzimidazolium salts and their Ag(I) complexes in the absence of oxidizing agent H_2O_2.

were found with late transition metal complexes used as DNA binding agents.[40]

DNA Binding Activity Using Viscosity Measurements

The binding nature of the benzimidazolium salts and their Ag complexes was further studied using viscosity measurements. This method is also a crucial tool to find the nature of binding of metal complexes to DNA.[41] The viscosity of DNA in a buffer solution is most sensitive to the changes in its effective length, and is one of the most significant tests for inferring the binding mode of compounds with DNA.[42] Plots of relative viscosity of complexes versus the ratio of concentration of complex and DNA are shown in Fig. 9. The relative viscosities of the complex-bound DNA solution

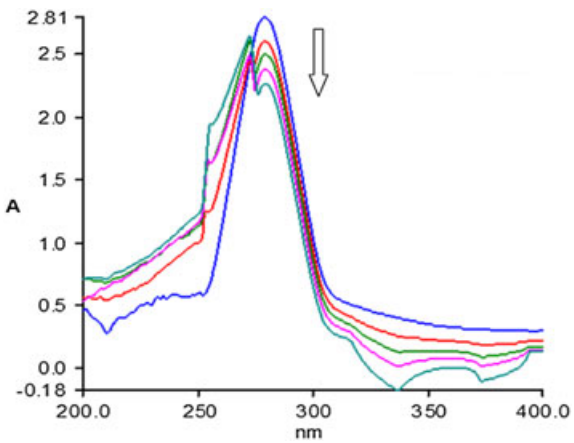

Figure 7. Absorption spectra of complex **10** in the presence of increasing amounts of *E. coli* gDNA. Arrow shows the absorption changes upon changing the DNA concentration.

increased with the concentration of complex tested (50–250 μl); hence an interactive mode of binding of complexes to DNA is assigned. Intercalative mode of binding of a compound to DNA is known to cause a significant increase in the viscosity of a DNA solution due to an increase in the separation of its base pairs at the intercalation site and, hence, an increase in the overall DNA molecular length.[43] Conversely, a compound that binds in the DNA grooves causes either a less pronounced change or no significant change in the viscosity of a DNA solution.

Conclusion

Four new non-symmetrically substituted nitrile-functionalized benzimidazolium salts and their Ag(I)– and Hg(II)–NHC complexes were prepared and characterized using different spectral and analytical techniques. All reported compounds were stable to air and moisture, and were readily soluble in polar and insoluble in non-polar organic solvents. Molecular structures of

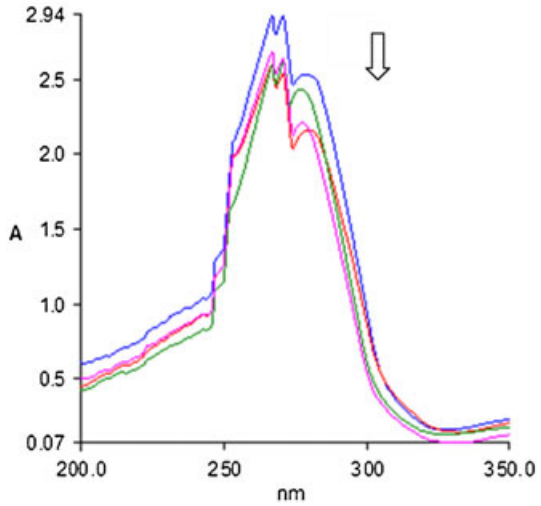

Figure 8. Absorption spectra of complex **16** in the presence of increasing amounts of *E. coli* gDNA. Arrow shows the absorption changes upon changing the DNA concentration.

Table 4. Intrinsic binding constants (K_b) of the benzimidazolium salts and Ag complexes

Sl no.	Compound	K_b
1	3	2.170×10^4
2	5	1.008×10^4
3	7	1.603×10^4
4	9	6.280×10^4
5	10	3.204×10^6
6	11	9.337×10^5
7	12	7.108×10^5
8	16	1.011×10^6

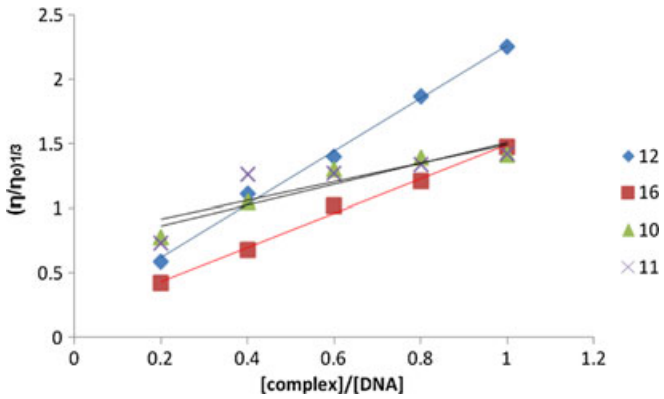

Figure 9. Effect of increasing concentration of Ag(I) complexes on the relative viscosities of *E. coli* gDNA at 30 °C.

benzimidazolium salts **2** and **5** were established using single-crystal X-ray diffraction methods. Benzimidazolium salts **5** and **9**, and Ag complex **16** showed moderate to significant DNA cleavage activity in the presence and absence of oxidizing agent. Additionally, investigation of UV–visible absorption spectral and viscosity measurement studies revealed the intercalative mode of binding of complexes with DNA with higher intrinsic binding constants. Further studies on the transmetallation of the newly synthesized complexes based on the literature method are underway.

Acknowledgements

R. A. Haque thanks Universiti Sains Malaysia (USM) for the short-term grant (203/PKIMIA/6311123) and the Research University (RU) grant 1001/PKIMIA/811217. S. Budagumpi thanks USM for a postdoctoral research fellowship.

References

[1] a) T. Dröge, F. Glorius, *Angew. Chem. Int. Ed.* **2010**, *49*, 6940. b) H. Clavier, S. P. Nolan, *Chem. Commun.* **2010**, *46*, 841. c) O. Kühl, *Coord. Chem. Rev.* **2009**, *253*, 2481. d) S. Díez-González, S. P. Nolan, *Coord. Chem. Rev.* **2007**, *251*, 874. e) L. Cavallo, A. Correa, C. Costabile, H. Jacobsen, *J. Organomet. Chem.* **2005**, *690*, 5407.
[2] a) M. Mooijman, E. Ruijter, A. H. Alberts, C. de Graaff, R. V. A. Orru, G. Rothenberg, *Appl. Organomet. Chem.* **2010**, *24*, 142. b) S. Budagumpi, R. A. Haque, A. W. Salman, *Coord. Chem. Rev.* **2012**, *256*, 1787.
[3] A. John, P. Ghosh, *Dalton Trans.* **2010**, *39*, 7183.
[4] H. V. Huynh, C. H. Yeo, Y. X. Chew, *Organometallics* **2010**, *29*, 1479.
[5] S. Patil, A. Deally, F. Hackenberg, L. Kaps, H. Müller-Bunz, R. Schobert, M. Tacke, *Helv. Chim. Acta* **2011**, *94*, 1551.
[6] S. Patil, A. Deally, B. Gleeson, H. Müller-Bunz, F. Paradisi, M. Tacke, *Appl. Organometal. Chem.* **2010**, *24*, 781.
[7] M. V. Baker, D. H. Brown, R. A. Haque, P. V. Simpson, B. W. Skelton, A. H. White, C. C. Williams, *Organometallics* **2009**, *28*, 3793.
[8] Q. X. Liu, L. N. Yin, X. M. Wu, J. C. Feng, *Polyhedron* **2008**, *27*, 87.
[9] K. M. Hindi, T. J. Siciliano, S. Durmus, M. J. Panzner, D. A. Medvetz, D. V. Reddy, L. A. Hogue, C. E. Hovie, J. K. Hilliard, R. J. Mallet, C. A. Tessier, C. L. Cannon, W. J. Youngs, *J. Med. Chem.* **2008**, *51*, 1577.
[10] S. Ray, R. Mohan, J. K. Singh, M. K. Samantaray, M. M. Shaikh, D. Panda, P. Ghosh, *J. Am. Chem. Soc.* **2007**, *129*, 15042.
[11] T. J. Siciliano, M. C. Deblock, K. M. Hindi, S. Durmus, M. J. Panzner, C. A. Tessier, W. J. Youngs, *J. Organomet. Chem.* **2011**, *696*, 1066.
[12] S. Berners-Price, R. Johnson, A. Giovenella, L. Faucette, C. Mirabelli, P. Sadler, *J. Inorg. Biochem.* **1988**, *33*, 285.
[13] H. Zhu, X. Zhang, X. Liu, X. Wang, G. Liu, A. Usman, H. Fun, *Inorg. Chem. Comm.* **2003**, *6*, 1113.
[14] M. Gottscaldt, A. Pfeifer, D. Koth, H. Gorls, H. Dahse, U. Mollmann, M. Obata, S. Yano, *Tetrahedron* **2006**, *62*, 11073.
[15] B. Thati, A. Noble, B. Creaven, M. Walsh, M. McCann, K. Kavanagh, M. Devereux, D. Egan, *Cancer Lett.* **2007**, *250*, 128.
[16] A. Gautier, F. Cisnetti, *Metallomics* **2012**, *4*, 23.
[17] A. F. Pozharskii, *Zh. Obshch. Khim.* **1964**, *34*, 630.
[18] a) G. M. Sheldrick, *Acta Cryst.* **2008**, *A64*, 112. b) A. L. Spek, *Acta Cryst.* **2009**, *D65*, 148.
[19] a) R. A. Haque, A. W. Salman, C. K. Whai, C. K. Quah, H.-K. Fun, *Acta Cryst.* **2011**, *E67*, m97. b) R. A. Haque, A. W. Salman, M. Hemamalini, H.-K. Fun, *Acta Cryst.* **2011**, *E67*, m1242.
[20] I. Özdemir, H. Arslan, S. Demir, D. VanDerveer, B. Çetinkaya, *Inorg. Chem. Commun.* **2008**, *11*, 1462.
[21] F. Li, J. J. Hu, L. L. Koh, T. S. Andy Hor, *Dalton Trans.* **2010**, *39*, 5231.
[22] A. R. Chianese, X. Li, M. C. Janzen, J. W. Faller, R. H. Crabtree, *Organometallics* **2003**, *22*, 1663.
[23] T. Ramnial, C. D. Abernethy, M. D. Spicer, I. D. McKenzie, I. D. Gay, J. A. C. Clyburne, *Inorg. Chem.* **2003**, *42*, 1391.
[24] B. E. Ketz, A. P. Cole, R. M. Waymouth, *Organometallics* **2004**, *23*, 2835.
[25] R. A. Haque, A. W. Salman, T. S. Guan, H. H. Abdallah, *J. Organomet. Chem.* **2011**, *696*, 3507.
[26] V. J. Catalano, M. A. Malwitz, *Inorg. Chem.* **2003**, *42*, 5483.
[27] U. M. Tripathi, A. Bauer, H. Schmidbaur, *J. Chem. Soc. Dalton Trans.* **1997**, 2865.
[28] J. C. C. Chen, I. J. B. Lin, *Organometallics* **2000**, *19*, 5113.
[29] S. Budagumpi, V. K. Revankar, *Transition Met. Chem.* **2010**, *35*, 649.
[30] S. Budagumpi, M. P. Sathisha, N. V. Kulkarni, G. S. Kurdekar, V. K. Revankar, *J. Incl. Phenom. Macrocycl. Chem.* **2010**, *66*, 327.
[31] S. B. Kalia, K. Lumba, G. Kaushal, M. Sharma, *Indian J. Chem.* **2007**, *46A*, 1233.
[32] W. J. Geary, *Coord. Chem. Rev.* **1971**, *7*, 81.

[33] R. A. Haque, M. A. Iqbal, S. Budagumpi, M. Hemamalini, H.-K. Fun, *Acta Cryst.* **2012**, *E68*, o573.
[34] R. A. Haque, M. A. Iqbal, S. A. Ahmad, T. S. Chia, H.-K. Fun, *Acta Cryst.* **2012**, *E68*, o845.
[35] J. K. Barton, A. T. Danishefsky, J. M. Goldberg, *J. Am. Chem. Soc.* **1984**, *106*, 2172.
[36] R. Barbieri, F. Huber, A. Silvestri, G. Ruisi, M. Rossi, G. Barone, A. B. Paulsen, *Appl. Organomet. Chem.* **1999**, *13*, 595.
[37] H. Liu, Y.-Y. Kou, L. Feng, D.-D. Li, C.-Y. Gao, J.-L. Tian, J.-Y. Zhang, S.-P. Yan, *Appl. Organomet. Chem.* **2010**, *24*, 636.
[38] a) S. Budagumpi, N. V. Kulkarni, G. S. Kurdekar, M. P. Sathisha, V. K. Revankar, *Eur. J. Med. Chem.* **2010**, *45*, 455. b) G. S. Kurdekar, S. M. Puttanagouda, N. V. Kulkarni, S. Budagumpi, V. K. Revankar, *Med. Chem. Res.* **2011**, *20*, 421.
[39] T. M. Kelly, A. B. Tossi, D. J. McConnell, T. C. Strekas, *Nucl. Acids Res.* **1985**, *13*, 6017.
[40] S. A. Tysoe, R. J. Morgan, A. D. Baker, T. C. Strekas, *J. Phys. Chem.* **1993**, *97*, 1707.
[41] S. Satyanarayana, J. C. Dabrowiak, J. B. Chaires, *Biochemistry* **1992**, *31*, 9319.
[42] R. Rao, A. K. Patra, P. R. Chetana, *Polyhedron* **2008**, *27*, 1343.
[43] J. M. Kelly, A. B. Tossi, D. J. McConnell, C. OhUigin, *Biochemistry* **1985**, *32*, 2573.

Appendix

CCDC 883342 and 883343 contain the supplementary crystallographic data for **2** and **5**, respectively. These data can be obtained free of charge via http://www.ccdc.cam.ac.uk/conts/retrieving.html, or from the Cambridge Crystallographic Data Centre, 12 Union Road, Cambridge CB2 1EZ, UK; fax: (+44) 1223-336-033; or e-mail: deposit@ccdc.cam.ac.uk.